Theoretical and Experimental Study on the Time−Dipole Correlation Function of 2-(Acetyloxy)ethyl-2-(2-naphthyl) Acetate (ANA)†

P. Saez-Torres,‡ E. Saiz,§ R. Díaz-Calleja,|| J. Guzmán,‡ and E. Riande*,‡

Instituto de Ciencia y Tecnología de Polímeros (CSIC), Madrid, Spain, Departamento de Qímica-Física, Universidad de Alcalá, 28871-Alcalá de Henares, Madrid, Spain, and Departamento de Termodinámica Aplicada, ETSII, UPV, 46071 Valencia, Spain

Received: February 2, 1998; In Final Form: April 16, 1998

The complex dielectric permittivity ϵ^* of the 2-(acetyloxy)ethyl-2-(2-naphthyl) acetate molecule, ANA, was measured as function of both temperature (in the range −130 to 0 °C) and frequency (from 10^{-4} to 10^2 kHz). Isochrone values of the loss component ϵ'' present a prominent peak with the maximum for 1 Hz located at −43 °C, close to the calorimetric value of T_g. Analysis of the temperature dependence of these absorptions allows the evaluation of the relative free volume of the sample at T_g as $\Phi_g/B = 0.026$. Molecular dynamics simulations seeking the evaluation of the time−dipole correlation function $\phi(t)$ including both auto- and cross-correlation terms were performed for a canonical ensemble of 15 molecules of ANA (i.e., 540 atoms) contained within a cubic box with periodic boundary conditions at constant temperature. Simulations were performed at $T = 300$, 500, 750, and 1000 K, and the results at 300 K indicate that the molecule does not statistically sample the whole conformational space during the time allowed to the simulation (i.e., 0.5 fs), so $\phi(t)$ was not computed at this temperature. The values of $\phi(t)$ obtained at the other three temperatures proved that the cross-correlation terms are negligible. Fitting of $\phi(t)$ to the KWW equation $\phi(t) = \exp[-(t/\tau)^{\bar{\beta}}]$ is very good, giving values of $\tau = 5.6$, 1.8, and 1.0 ps, respectively, for $T = 500$, 750, and 1000 K, while $\bar{\beta} = 0.65 \pm 0.02$ is temperature independent. Values of ϵ' (real) and ϵ'' (loss) components of ϵ^* computed with these values of $\phi(t)$ are in good agreement with experimental results.

Introduction

Condensed phases, either liquid, glassy, or crystalline, are the result of interactions among atoms, ions, or molecules. Obviously the type and intensity of the interactions depend on the chemical structure of the condensed phases. When a noncrystallizable liquid is cooled, a temperature is reached at which the mechanisms that keep the liquid structure at equilibrium are associated with times that are larger than the time scale of the experiment,[1,2] however large this time scale is. This temperature is the so-called glass transition temperature T_g. The glass transition is manifested by a sharp decrease of the heat capacity C_p from liquidlike to crystallike values because in this situation the system has only kinetic accessibility to a small fraction of the available conformational space during the time scale of the experiment. Though there is not an international convention to define the glass transition temperature, this magnitude is often taken as the temperature at the onset of the increase in C_p during heating,[2] usually at 10 K/min. Dramatic changes occur in the physical properties during the glass → liquid transition. Compliance magnitudes such as the creep compliance and dielectric permittivity undergo a sharp decrease in the transition from liquid to glass, while both the mechanical and the dielectric relaxation moduli experience an abrupt increase. Mechanical and dielectric loss functions present a prominent peak at the glass transition temperature.[3]

The isochrones showing the temperature dependence of mechanical or dielectric loss functions present in the glassy state a relatively weak absorption associated with local motions, called the β process, followed in increasing order of temperature by a prominent absorption associated with the glass−liquid transition, named the α relaxation, presumably produced by generalized micro-Brownian motions. The fact that the β and the α relaxations do not show molecular weight dependence for long chains[4−6] suggests some sort of cooperativity in the molecular motions that produce these relaxations. High molecular weight chains display an additional relaxation, associated with motions of the whole chain, at temperatures above T_g. This relaxation, also called the normal mode process, is observed in the mechanical relaxation spectra of amorphous polymers.[4,7] However, the normal mode in the dielectric spectra is only observed when the dipole moment is along the chain contour.[5,8] Obviously, the isochrones corresponding to low molecular compounds only exhibit the β and the α absorptions.

The relaxation spectra of condensed amorphous substances in the frequency domain at temperatures above T_g present the same absorptions appearing in the isochrones. At high frequencies (short times) the β absorptions appear followed, in decreasing order of frequency, by the α and the normal mode relaxation processes. The α relaxation inevitably displays a Kohlrausch−Williams−Watts (KWW) "stretch exponential" decay[9−11]

$$\phi(t) = \exp\left[-\left(\frac{t}{\tau^*}\right)^{\bar{\beta}}\right] \qquad (1)$$

where $1 \geq \bar{\beta} > 0$ and τ^* is a characteristic or mean-relaxation

† This paper is dedicated to the memory of Professor Irmina Hernandez-Fuentes.
‡ CSIC.
§ Universidad de Alcalà.
|| ETSII.

S1089-5639(98)00973-6 CCC: $15.00
Published on Web 06/20/1998

time, somewhat dependent on the type of response, defined by the area under the curve of $\phi(t)$. In the vicinity of T_g, the parameter τ^* commonly undergoes a rapid rise with declining temperature, which often fits to a Vogel−Tamman−Fulcher−Hesse (VTFH) form[12−14]

$$\tau^* = \tau_0 \exp\left[\frac{A}{T - T_\infty}\right] \tag{2}$$

where τ_0 is in the range of picoseconds and T_∞ is believed to be related to the Kauzmann temperature,[2] that is, the temperature at which the conformational entropy is zero. The system falls out of equilibrium if τ^* is larger than the time scale of the experiment.

The dielectric relaxation spectra of flexible molecules with dipoles either perpendicular to the chain contour or located in flexible side groups only present the β and α relaxations. In the cases in which the β process is negligible in comparison with the α relaxation, the KWW decay function at $T > T_g$ can be expressed in molecular terms by the following expression[15,16]

$$\phi(t) = \frac{\langle \mu_i(t)\cdot\mu_i(0)\rangle + \sum_{i\neq j}\langle \mu_i(t)\cdot\mu_j(0)\rangle}{\langle \mu_i^2\rangle + \sum_{i\neq j}\langle \mu_i(0)\cdot\mu_j(0)\rangle} \tag{3}$$

where $\phi(t)$ can then be called the time−dipole correlation function, $\mu_i(t)$ is the dipole moment of the molecule i at time t, and brackets mean averages.

Molecular dynamics (MD) simulations have been used to determine the dielectric properties of model compounds of flexible side groups of polymers, specifically the mean-square dipole moment $\langle \mu^2 \rangle$ of esters containing cycloaliphatic rings in their structure.[17,18] MD simulations were also employed to calculate the normalized components of the complex dielectric permittivity of these compounds in the frequency domain.[19−21] However, only auto-correlation terms were used in the former calculations of $\phi(t)$. In this work, we simulate $\phi(t)$ for 2-(acetyloxy)ethyl-2-(2-naphthyl) acetate, ANA, model compound of poly(2-{[2-(2-naphthyl)acetyl]oxy}ethyl) acrylate, taking into account both auto- and cross-correlation contributions. This paper reports the behavior of cross-correlation functions for the first time to our knowledge. From the simulated values of $\phi(t)$, the normalized components of the complex dielectric permittivity of the model compound will be evaluated and the results obtained compared with the experimental ones. This study forms part of a project devoted to the simulation of the dielectric relaxation behavior of molecular chains as function of their structure.

Experimental Part

2-Hydoxyethyl-2-(2-naphthyl) acetate (HNA) was synthesized by reaction of naphthyl acetic acid (NAA) with ethylene glycol (EG). The esterification was carried out in refluxing toluene, under a nitrogen atmosphere, using a molar ratio NAA/EG = 35/88 and *p*-toluenesulfonic acid as catalyst. Water produced in the esterification reaction was eliminated with a Dean−Stark distillation trap. The esterification proceeded for 24 h, and then the toluene in the reaction medium was separated at reduced pressure. HNA was separated from the ethylene glycol dinaphthyl acetate formed in the reaction in successive silica gel columns using the following eluents: hexane−ethyl acetate (3:1), hexane−ethyl acetate (2:1), and hexane−ethyl acetate (1:1). A second esterification reaction was performed by dropwise addition of acetyl chloride to a benzene solution of HNA in benzene containing triethylamine, Et_3N. The HCl formed in the reaction was neutralized with Et_3N. The reaction medium was washed three times with water, and the organic phase was separated. Also the aqueous phase was extracted with benzene to remove the organic product present in this phase, and the organic phase was added to the first set. The organic phase was dried with sodium sulfate and filtered, and the solvent was separated under reduced pressure. The product, 2-(acetyloxy)-ethyl-2-(2-naphthyl) acetate (ANA), was purified using a silica gel column and hexane−ethyl acetate (4:1) as eluent. The purity of the product was checked by ^{1}H NMR and ^{13}C NMR spectroscopies.

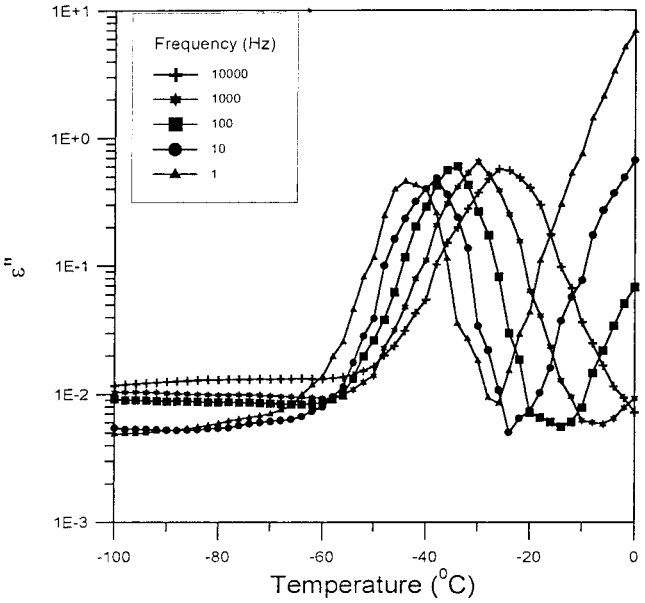

Figure 1. Temperature dependence of the dielectric loss ϵ'' for 2-(acetyloxy)ethyl-2-(2-naphthyl)acetate (ANA) at the frequencies indicated.

The components ϵ' and ϵ'' of the relative permittivity ϵ^* of ANA were measured with a capacitance apparatus TA-DEA 2970, from TA Instruments, operating in the frequency range $10^{-4}-10^2$ kHz. In the glassy region the measurements were made from low to high temperature at a heating rate of 1 °C/min. In the glass → liquid transition, ϵ' and ϵ'' were measured under isothermal conditions at steps of 5 °C. The error involved in the measurements of ϵ' and ϵ'' was estimated to be lower than 5%.

The glass transition temperature was determined with a DSC-7 Perkin-Elmer calorimeter, at a heating rate of 10 K/min. The T_g, taken on the onset of the increase of specific capacity during heating, was −41 °C.

Experimental Results

Illustrative curves showing the temperature dependence of the dielectric loss ϵ'' for the ANA molecule are plotted at several frequencies in Figure 1. The isochrones present a prominent absorption corresponding to the glass−liquid transition or α relaxation process. The maximum of the absorption peak of the isochrone at 1 Hz is located at −43 °C, close to the calorimetric glass transition temperature. As usual, the maximum of the peaks are shifted to higher temperatures with increasing frequency. Subglass absorptions were not detected in the glassy region down to −130 °C. The α relaxation can also be observed when the dielectric loss is represented in the frequency domain, at temperatures slightly higher than T_g.

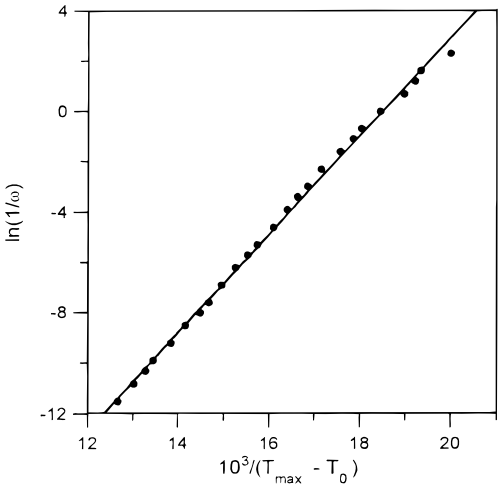

Figure 2. Natural logarithm of the reciprocal of the experimental frequencies versus the reciprocal of $T_{max} - T_\infty$, where T_{max} is the temperature at which the maximum of ϵ'' is reached for each frequency while T_∞ was taken to be $T_g - 50$.

The mean relaxation times associated with the α process is usually taken are the reciprocal of $2\pi f$ at the peak maximum, where f is the frequency in Hz. Doolittle formulated the following empirical equation for the relaxation times[22]

$$\tau = A \exp\left[\frac{B}{\Phi}\right] \tag{4}$$

where Φ is the relative free volume and B is believed to be related to the ratio between the volume necessary for a relaxation process to take place and the volume of the segment or segments intervening in the relaxation.[23] The assumption that the volume is a linear function of temperature leads eq 4 to the Vogel−Fulcher−Tamman−Hess (VTFH) expression (eq 2). By comparing eqs 2 and 4 the following relationship is obtained

$$\frac{\Phi_g}{B} = \frac{T_g - T_\infty}{m} \tag{5}$$

This expression permits one to obtain the relative free volume at T_g. The values of m and T_∞ in eq 5 were obtained by plotting the natural logarithm of the relaxation times against $1/(T_{max} - T_\infty)$, as eq 2 suggests. The value of T_∞ was set 50 K below the calorimetric T_g (i.e., $T_\infty = 176$ K). The plot, shown in Figure 2, fits to a straight line with a slope $m = 1950$ from which one obtains $\Phi_g/B = 0.026$. It is noteworthy that the result obtained for Φ_g/B lies in the range 0.025 ± 0.005 reported for viscoelastic liquids.[4]

For Debye type substances, that is, for systems whose responses are described by a single relaxation time, the complex plane plots ϵ'' against ϵ' are semicircumferences whose intercepts with the abscissas axis give, respectively, the relaxed ϵ_0 [$=\epsilon'(0)$] and unrelaxed ϵ_∞ [$=\epsilon'(\infty)$] permittivities. In general the dielectric relaxation behavior of liquids cannot be described by a single relaxation time, and the complex plane plots are arcs that eventually become skewed arcs in polymers and other complex liquids in which the α relaxation has a wide distribution of relaxation times. In general these curves fit to the Havriliak−Negami (HN) equation[24,25]

$$\epsilon^*(\omega) = \epsilon_\infty + \frac{\epsilon_0 - \epsilon_\infty}{[1 + (i\omega\tau_0)^{1-\bar{\alpha}}]^{\bar{\gamma}}} \tag{6}$$

where $0 \le \bar{\alpha} < 1$ and $0 \le \bar{\gamma} < 1$. For a Debye type relaxation

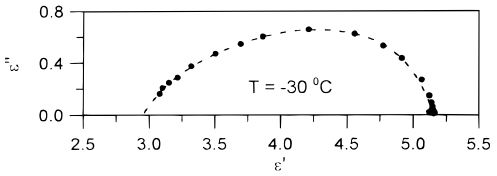

Figure 3. Complex plane representation of ϵ^* (i.e., loss ϵ'' versus real ϵ' components) for the ANA molecule at −30 °C.

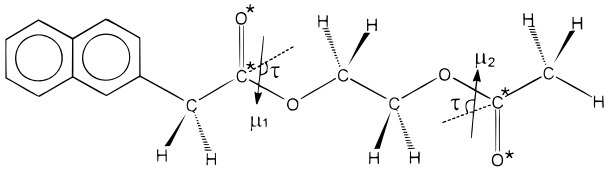

Figure 4. Planar all-trans conformation of the ANA molecule. Rotational angles were taken to be 180° for this orientation. Approximate directions of the dipole moments of the two ester groups are represented by arrows. They are shown only for illustrative purposes since all calculations were performed employing partial charges assigned to every atom of the molecule.

$\bar{\alpha} = 0$ and $\bar{\gamma} = 1$. Consequently, the larger is the departure of $\bar{\alpha}$ and $\bar{\gamma}$ from 0 and 1, respectively, the higher is the complexity of the system.

An illustrative plot for the dielectric results of ANA at −30 °C is shown in Figure 3. It can be seen that the curve is a skewed arc whose HN parameters are as follows: $\epsilon'_0 = 5.16$; $\epsilon'_\infty = 2.95$; $\bar{\alpha} = 0.72$; $\bar{\gamma} = 0.016$ and $\tau_0 = 2.5 \times 10^{-3}$ s ($2\pi\tau_0 = 1.6 \times 10^{-2}$ s).

Theoretical Analysis

Molecular dynamic (MD) simulations were performed according to standard procedures[26] with the DL_POLY package[27] employing the Amber force field.[28−30] A time step $\delta = 1$ fs (i.e., 10^{-15} s) was used for the integration cycle. No scaling of the 1−4 interactions was performed. The Coulombic term of the potential energy was computed as the sum of pairwise interactions among partial charges assigned to every atom on the sample by means of the AMPAC program and the AM1 procedure.[31] The same charges were employed to compute dipole moments of every conformation adopted by the molecules of the system along the MD trajectories. The temperature of the sample was controlled by scaling the atomic velocities after each integration cycle with a damping factor of 1000 fs in order to allow relatively high thermal fluctuations that will facilitate the passage over energy barriers.[32]

A canonical ensemble (i.e., constant T, V, N) of 15 molecules (i.e., 540 atoms) of ANA, whose structure is represented in Figure 4, contained into a cubic box with periodic boundary conditions was employed for all the theoretical calculations. The side of the box was set to $L = 18.9$ Å in order to produce a density of 1 g/cm^3. The system was initially built within a much larger box with $L_0 = 26.9$ Å with one molecule placed at the center of the cube and the other 14 located close to the vertexes and centers of the faces in order to avoid interpenetration among different molecules, which would produce unrealistically high values of energy thus rendering difficult and unreliable any conceivable strategy for energy minimization. A MD simulation at high temperature (i.e., 1000 K) was then applied to this initial system, and the side of the box was decreased from the initial value L_0 to the final length L with increments of −0.2 Å and allowing a relaxation time of 500 fs at each new size. Once the final volume was obtained, the system was cooled to 50 K, with increments of −50 K and allowing relaxation times of 500

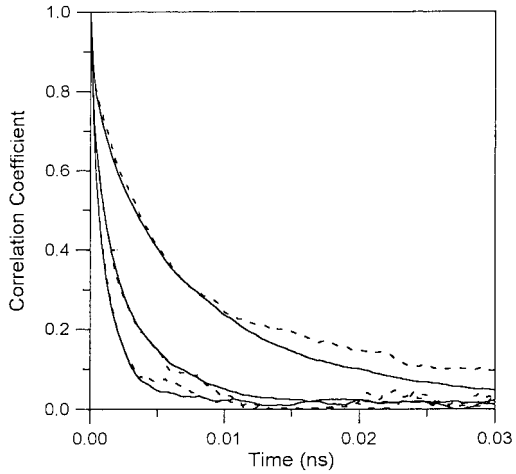

Figure 5. Dipole correlation coefficients $\phi_f(t)$ (full-correlation including cross-correlation terms) and $\phi_a(t)$ (auto-correlation obtained by neglecting the cross-correlation terms) as function of time for the ANA molecule obtained at temperatures of 500, 750, and 1000 K (from top to bottom). Solid lines represent values $\phi_a(t)$, while broken lines represent $\phi_f(t)$.

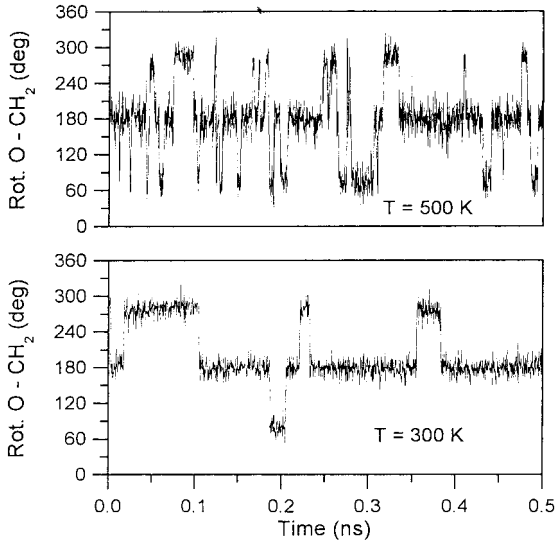

Figure 6. Evolution with time of the rotational angle over the O−CH_2 bond of the ANA molecule obtained at 300 and 500 K.

fs at each new temperature, to minimize the energy and finally warmed to the working temperature, again with increments of 50 K and relaxation times of 500 fs. After all this preparation, the data collection process was started. Thus, a MD simulation of 5×10^5 steps, covering a total time span of 0.5 ns, was carried out saving the coordinates of all the atoms in the system every $\Delta = 200$ fs, thus producing $N = 2500$ conformations that were employed in posterior analysis. It is obvious that any increase in either the size of the sample (i.e., the number of molecules within the box), the length of the MD trajectories or both features at the same time may improve the reliability of the results. Unfortunately, the required computer time also increases with both characteristics (especially with the number of atoms in the sample), so that a compromise should be reached. The size of the sample employed in this work is reasonable, since if we imagine one molecule placed at the center of the repeating cell, all the first neighbor molecules surrounding it, which presumably produce the strongest interactions, are placed in the same cell. On the other hand, provided that the MD simulations are performed at high temperatures, 0.5 ns is a large enough time span as to allow many conformational transitions during

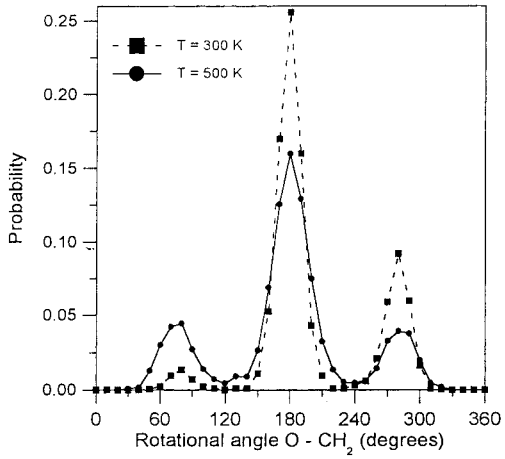

Figure 7. Probability distribution of the values for the rotation over the O−CH_2 bond of the ANA molecule computed at 300 and 500 K.

the MD trajectory, so that the molecules may statistically sample their whole conformational space.

Calculations were performed at four temperatures, namely, 300, 500, 750, and 1000 K. At each of these temperatures, the dipole moment of every individual ANA molecule on the ensemble was computed as function of time for the N conformations recorded during the MD simulation. These dipoles are represented as $\mu_i(k\Delta)$ with $i = 1-15$ representing the molecules on the ensemble, $k = 0-2499$ indicating the conformation, and $\Delta = 200$ fs being the time gap between consecutive conformations, so that $k\Delta$ represents a value of time. Dipole moments thus obtained were employed to compute full- and auto-correlation coefficients that will be represented as $\phi_f(t)$ and $\phi_a(t)$ according to the expressions

$$\phi_f(n\Delta) = \frac{1}{N-n}\sum_{k=1}^{N-n} \times \left[\frac{\langle \mu_i(k\Delta)\,\mu_i[(k+n)\Delta]\rangle + \langle \sum_{i\neq j}\mu_i(k\Delta)\,\mu_j[(k+n)\Delta]\rangle}{\langle \mu_i(k\Delta)\,\mu_i(k\Delta]\rangle + \langle \sum_{i\neq j}\mu_i(k\Delta)\,\mu_j(k\Delta)\rangle}\right] \quad (7)$$

$$\phi_a(n\Delta) = \frac{1}{\langle \mu^2\rangle\,(N-n)}\langle \sum_{k=1}^{N-n}\mu[k\Delta]\cdot\mu[(k+n)\Delta]\rangle \quad (8)$$

where the angle brackets represent averages over the 15 molecules contained in the ensemble and ϕ_a is obtained from ϕ_f by neglecting the cross-correlation terms in which $i \neq j$.

In fact, these equations represent an average over the $N - n$ values of ϕ obtained with all the pairs of conformations that are separated by a time equal to $n\Delta$, The value of the correlation function decreases rather fast with increasing time; thus, $\phi(n\Delta) \approx 0$ for values of n that are much smaller than the total number of studied conformations N and therefore $N - n$ is very large, which ensures a good sampling of ϕ over all the conformational space.[19]

The results obtained at 500, 750, and 1000 K are shown in Figure 5 where solid/broken lines represent values of ϕ_a/ϕ_f. As can be seen in this figure, cross-correlation terms are quite negligible. The values computed at 300 K are not included in Figure 5 since at this temperature the molecules do not statistically sample their whole conformational space during the time allowed to the MD simulation as is illustrated in Figures 6 and 7 that represent, respectively, the evolution with time of

TABLE 1: Coefficients for the Best Fit of the Correlation Factors g_f (Cross-Correlation Terms Included) and ϕ_a (Cross-Correlation Terms Neglected) Obtained at Different Temperatures by MD Simulations to the KWW Equation $\phi(t) = \exp[-(t/T)^{\bar\beta}]$[a]

		$T = 500$ K	$T = 750$ K	$T = 1000$ K
ϕ_f	$10^3\tau$ (ns)	6.2	1.7	1.0
	$\bar\beta$	0.58	0.64	0.65
	$10^3\sigma^2$	0.2	0.3	0.4
ϕ_a	$10^3\tau$ (ns)	5.6	1.8	1.0
	$\bar\beta$	0.65	0.63	0.67
	$10^3\sigma^2$	0.06	0.1	0.2

[a] The sum of the squared deviations on the fitting is represented by σ^2.

the rotational angle χ over the O−CH_2 bond and the probability of finding a given value of χ within the MD trajectory computed at 300 and 500 K for one of the molecules contained in the ensemble. The results obtained at 300 K indicate that the conformational transitions are slow at this temperature and, as consequence, the probability of finding gauche states (i.e., $\chi \approx \pm 60°$) is not the same for both of them as the symmetry of the molecule dictates. On the contrary, the transitions are faster at 500 K and the molecule visits both gauche states roughly with the same probability, although trans is still the preferred orientation for this bond.

According to the phenomenological linear theory of dielectrics, transformation of $\phi(t)$ from the time domain to the frequency domain gives the complex permittivity according to the following equation[11]

$$\frac{\epsilon^*(\omega) - \epsilon_\infty}{\epsilon_0 - \epsilon_\infty} = 1 - \int_0^\infty \phi(t)\exp(-i\omega t)\,dt \qquad (9)$$

To eliminate noises and facilitate further treatment of data, the values of $\phi(t)$ were fitted to the KWW function[9−11] (eq 1). The coefficients obtained in the fitting are summarized in Table 1. The sum of the squared deviations obtained, also shown in Table 1, indicates that the fitting is much better in the case of auto- than in full-correlation coefficients. This difference could also be appreciated in Figure 5, which shows that the values of $\phi_f(t)$ and $\phi_a(t)$ computed at the same temperature are almost identical at short times and differ at higher times, mainly due to noise fluctuations of $\phi_f(t)$. As expected, the results of Table 1 show that the mean-relaxation time τ^* decreases with increasing temperature, while β is roughly temperature-independent with a value of $\beta = 0.65 \pm 0.02$.

Substitution of eq 1 into eq 9 leads to a series expansion for the integrals that only depends on the value of β[11]

$$\frac{\epsilon^*(\omega) - \epsilon_\infty}{\epsilon_0 - \epsilon_\infty} = \sum_{n=1}^{\infty}\frac{(-1)^{n-1}}{(\omega\tau_0)^{n\bar\beta}}\frac{\Gamma(n\bar\beta+1)}{\Gamma(n+1)}\left[\cos\left(\frac{n\bar\beta\pi}{2}\right) - i\sin\left(\frac{n\bar\beta\pi}{2}\right)\right] \qquad (10)$$

for high frequencies (i.e., $-1 \le \log(\omega\tau_0) \le +4$ when $\bar\beta > 0.25$), and

$$\frac{\epsilon^*(\omega) - \epsilon_\infty}{\epsilon_0 - \epsilon_\infty} = \sum_{n=1}^{\infty}(-1)^{n-1}\frac{(\omega\tau_0)^{n-1}}{\Gamma(n)}\Gamma\left(\frac{n+\bar\beta-1}{\bar\beta}\right)\times \left[\cos\left(\frac{(n-1)\pi}{2}\right) + i\sin\left(\frac{(n-1)\pi}{2}\right)\right] \qquad (11)$$

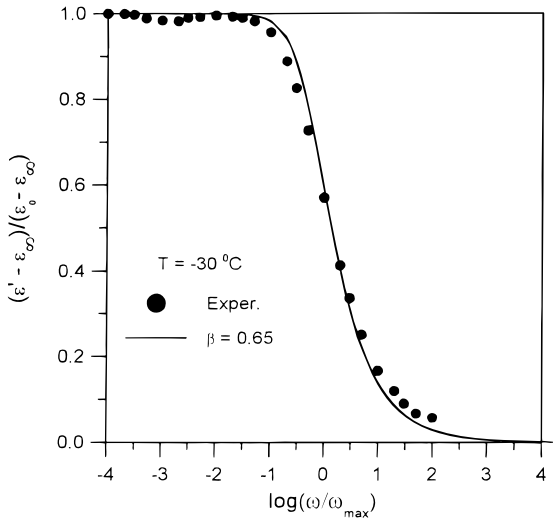

Figure 8. Normalized values of the real component ϵ' of the complex dielectrical permittivity ϵ^* of ANA. The circles represent experimental values measured at −30 °C, while the line indicates theoretical results computed with the value $\bar\beta = 0.65$.

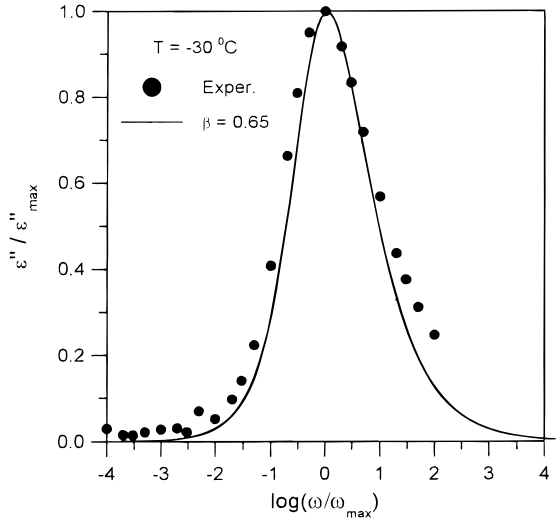

Figure 9. Same as Figure 8 for the loss component ϵ''.

for low frequencies. Figures 8 and 9 present the theoretical values of both the normalized loss and real components of the complex permittivity computed according to eq 10 for $\bar\beta = 0.65$ as a function of $\log(\omega/\omega_{max})$ together with the experimental results of these magnitudes. It can be seen in these figures that the theoretical calculations are in reasonable agreement with the experimental results.

Discussion

Previous calculations[32] proved that, at 30 °C, an isolated ANA molecule can visit the whole conformational space in about 10 ns. Thus, the value of the mean-square dipole moment $\langle\mu^2\rangle$ calculated from the evolution of the trajectory of μ^2 in the conformational space is 5.7 D^2, in rather good agreement with the experimental result,[32] 5.3 D^2. The analysis of the MD trajectories shows that the plane defined by the pair of bonds C^{ar}−CH_2−C* is roughly perpendicular to the aromatic group while trans orientation of the CH_2−C* bond is disfavored by ca. 1.5 kcal mol^{-1} vs gauche. In the O−CH_2−CH_2−O segment, trans states about O−CH_2 bonds are preferred by ca. 1.2 kcal mol^{-1} over the alternative gauche states while gauche states about CH_2−CH_2 bonds have an energy 0.9 kcal mol^{-1} below

that of the alternative trans state. It is noteworthy that second-order interactions controlling the stability of opposite and identical combinations of gauche states over the pair of bonds $O-CH_2-CH_2$ are both negative.[32]

The relaxation of the complex permittivity of the condensed matter in the bulk arises from a weighted sum of cross-correlated and auto-correlated terms. It has been reasoned that though cross-correlation contributions may have a significant magnitude, its time dependence may be similar to that of the auto-correlation function. In other words, cross-correlation terms, although present, may not significantly affect the time dependence of the decay function.[16] This assumption is supported by the values of $\bar{\beta}$ computed at different temperatures and given in Table 1. It can be seen that the value of $\bar{\beta}$ is nearly the same for the auto- and the full time−dipolar correlation coefficients. Moreover, as shown in Figures 8 and 9, the simulations reproduce rather well the experimental results, though to get an optimum fit would require a value of $\bar{\beta}$ in the vicinity of 0.60. Therefore the simulation of the time−dipolar correlation coefficient for isolated molecules may be sufficient to describe the α relaxation of the amorphous condensed matter. Actually, earlier work[19−21] carried out on the simulation of the α dielectric relaxation of flexible esters containing substituted cyclohexane and 1,3-dioxane rings in their structure has shown that the time−dipole correlation coefficient of isolated molecules gives a good account of the dynamic dielectric properties of these molecules in the bulk.

A shortcoming of the MD simulations at the present stage is that the evaluation of the time−dipole correlation coefficient within a reasonable computing time requires the use of unrealistically high temperatures. Consequently, the extrapolation of the values of the mean-relaxation time to temperatures close to T_g is not possible, and consequently, information concerning the parameters of the VFTH equation cannot be obtained from the simulations. However, the fact that the simulated relaxations match the experimental results obtained at temperatures close to T_g suggests that the time−temperature correspondence principle holds in these cases. In support of this assumption it should be noted that recent experimental work seems to indicate that the stretch exponent of the decay function for the α relaxation of some polymers seems to be independent of temperature.[33−34] Obviously, this only occurs in the case that the strength of the β process is negligible in comparison with that of the α relaxation. Otherwise, as the temperature increases both the α and β relaxations are shifted to higher frequencies. Because the activation energy of the α relaxation is significantly larger than that of the β process, a temperature can be reached at which both relaxations overlap forming the $\alpha\beta$ relaxation[16] whose stretch exponent in eq 2 will differ from that of the α. In this case, the time−temperature correspondence will not hold.

Acknowledgment. This work was supported by the DGICYT through Grants PB94-0364 and PB96-0134-C02-01

References and Notes

(1) Stillinger, F. H. *Science* **1995**, *267*, 1935.
(2) Angel, C. A. *Science* **1995**, *267*, 1995.
(3) McCrum, N. G.; Read, B. E.; Williams, G. *Anelastic and Dielectric Effects in Polymeric Solids*; Wiley: London, 1967 and Dover Publishers, New York, 1991.
(4) Ferry, J. D. *Viscoelastic Properties of Polymers*, 3rd ed.; Wiley-Interscience: New York, 1980.
(5) Stockmayer, W. H. *Pure Appl. Chem.* **1967**, *15*, 539.
(6) Block, H. *Adv. Polym. Sci.* **1979**, *33*, 93.
(7) Doi, M.; Edwards, S. F. *Theory of Liquids*; Clarendon Press: London, 1986.
(8) Adachi, K. Dielectric Relaxation in Polymer Solutions. In *Dielectric Spectroscopy in Polymeric Materials*; Runt, J. P., Fitzgerald, J. J., Eds.; American Chemical Society: Washington DC, 1997.
(9) Kohlrausch, F. *Ann. Phys. (Leipzig)* **1854**, *91*, 56, 179; **1863**, *4*, 337; **1866**, *8*, 1.
(10) Williams, G.; Watts, D. C. *Trans. Faraday Soc.* **1970**, *66*, 80.
(11) Williams, G.; Watts, D. C.; Dev, S. B.; North, A. M. *Trans. Faraday Soc.* **1971**, *67*, 1323.
(12) Vogel, H. *Z. Phys.* **1921**, *22*, 645.
(13) Fulcher, G. S. J. *Am. Ceram. Soc.* **1925**, *8*, 339.
(14) Tamman, G.; Hesse, W. *Z. Anorg. Allg. Chem.* **1926**, *156*, 245.
(15) Williams, G. *Chem. Rev.* **1972**, *72*, 55.
(16) Williams, G. *Dielectric Spectroscopy of Amorphous Polymer Systems: The Modern Approaches* in *Keynote Lectures in Selected Topics of Polymer Science;* Riande, E., ed; CSIC: Madrid, 1995.
(17) Saiz, E.; Riande, E. *J. Chem. Phys.* **1995**, *103*, 3832.
(18) Saiz, E.; Riande, E.; Guzmán, J.; Iglesias, M. T. *J. Phys. Chem.* **1996**, *100*, 3818.
(19) Saiz, E.; Riande, E.; Díaz-Calleja, R. *J. Phys. Chem. A* **1997**, *101*, 7324.
(20) Saiz, E.; Riande, E.; Díaz-Calleja, R.; Guzmán, J. *J. Phys. Chem. B* **1997**, *101*, 10949.
(21) Saiz, E.; Riande, E.; Díaz-Calleja, R. *J. Chem. Soc., Perkin Trans. 2* **1998**, 277.
(22) Doolitle, A. K.; Doolittle, D. B. *J. Appl. Phys.* **1957**, *28*, 901.
(23) Turnbull, D. C.; Cohen, M. H. *J. Chem. Phys.* **1958**, *29*, 1049.
(24) Havriliak, S.; Negami, S. *Polymer* **1967**, *8*, 161; **1969**, *10*, 859.
(25) Havriliak, S., Jr.; Havriliak, S. J. *Dielectric and Mechanical Relaxation in Materials*; Carl Hanser Verlag: New York, 1997.
(26) Allen, M. P.; Tildesley, D. J. *Computer Simulation of Liquids*; Clarendon Press: Oxford, 1987.
(27) Forester, T. R.; Smith, W. *DL_POLY* (Ver. 2.0); Daresbury Laboratory: Daresbury, Warrington WA4 4AD, England.
(28) Weiner, S. J.; Kollman, P. A.; Case, D. A.; Singh, U. C.; Ghio, C.; Alagona, G.; Profeta, S., Jr.; Weiner, P. *J. Am. Chem. Soc.* **1984**, *106*, 765.
(29) Weiner, S. J.; Kollman, P. A.; Nguyen, D. T.; Case, D. A. *J. Comput. Chem.* **1986**, *7*, 230.
(30) Homans, S. W. *Biochemistry* **1990**, *29*, 9110.
(31) MOPAC, *Quantum Chemistry Program Exchange*; Department of Chemistry, Indiana University: Bloomington, IN.
(32) Saez-Torres, P.; Tarazona, M. P.; Saiz, E.; Riande, E.; Guzmán, J. *J. Chem. Soc., Perkin Trans. 2* **1998**, 31.
(33) Behrens, C. F.; Christiansen, T. G.; Christensen, T.; Dyre, J. C.; Olsen, N. B. *Phys. Rev. Lett.*, **1996**, *76*, 1553
(34) Olsen, N. B. *Abstracts of the 3rd International Discussion Meeting on Relaxations in Complex Systems*, Vigo, Spain, 1997; Oral Commun. no. 14.